Shaw et al. *Boundary Value Problems* (2016) 2016:2
DOI 10.1186/s13661-015-0506-2

Boundary Value Problems
a SpringerOpen Journal

RESEARCH Open Access

Effects of slip on nonlinear convection in nanofluid flow on stretching surfaces

Sachin Shaw[1], Peri K Kameswaran[1,2] and Precious Sibanda[1*]

*Correspondence:
sibandap@ukzn.ac.za
[1]School of Mathematics, Statistics and Computer Science, University of KwaZulu-Natal, Private Bag X01 Scottsville, Pietermaritzburg, 3209, South Africa
Full list of author information is available at the end of the article

Abstract

We investigate the effects of momentum, thermal, and solute slip boundary conditions on nanofluid boundary layer flow along a permeable surface. The conventional no-slip boundary conditions at the surface are replaced by slip boundary conditions. At moderate to high temperatures, the temperature-concentration dependence relation is nonlinear and the Soret effect is significant. The governing partial differential equations are solved numerically. The influence of significant parameters on the fluid properties as well as on the skin friction, local Nusselt number, local Sherwood number, and the local nanoparticle Sherwood number are determined. We show, among other results, that the existence and uniqueness of the solutions depends on the slip parameters, and that the region of existence of the dual solution increases with the slip parameters.

Keywords: stagnation-point flow; nonlinear convection; partial slip; dual solutions; Soret effect

1 Introduction

Boundary layer flow over a stretching surface is important as it occurs in several engineering process, for example, materials manufactured by extrusion. During the manufacturing process, a stretching sheet interacts with the ambient fluid both thermally and mechanically. Several studies on the dynamics of boundary layer flow over a stretching surface have appeared in the literature (Crane [1]; Dutta *et al.* [2]). Recently an innovative technique used for improving heat transfer is to add ultra fine solid particles to a base fluid, Choi [3]. Recent literature shows a significant rise in applications of nanofluids such as in microchannels (Ebrahimi *et al.* [4], enzyme biosensors (Li *et al.* [5]), drug delivery (Shaw and Murthy [6]) biomimetic microsystems (Huh *et al.* [7]) etc. An impressive review of nanofluid research is given by Das *et al.* [8]. Kameswaran *et al.* [9] studied homogeneous-heterogeneous reactions in a nanofluid flow over a porous stretching sheet. Mabood *et al.* [10] studied the MHD boundary layer flow of nanofluids over a nonlinear stretching sheet.

A significant number of studies have applied the no-slip boundary conditions at the wall. However, the no-slip assumption is not applicable when fluid flows in micro and nano channels and must be replaced by slip boundary conditions (Aziz [11]). Nield and Kuznetsov [12] presented an analytic solution for convection flow in channel or circular ducts saturated with a rarefied gas in a slip-flow regime. The slip condition applies to corner flows and in the extrusion of polynomial melts from a capillary tube (Thompson

and Troian [13]; Nguyen and Wereley [14]). Karniadakis *et al.* [15] showed that hydrodynamic and thermal slip occur simultaneously. The difference between the fluid velocity at the wall and the velocity of the wall itself is directly proportional to the shear stress. The proportionality constant is called the slip length (Maxwell [16]; Hak [17]).

Beavers and Joseph [18] investigated fluid flow over a permeable wall with a slip boundary condition. The effects of a second order velocity-slip and temperature-jump on basic gaseous fluctuating micro-flows were analyzed by Hamdan *et al.* [19]. The effects of partial slip on steady boundary layer stagnation-point flow of an incompressible fluid and heat transfer from a shrinking sheet was investigated by Bhattacharyya *et al.* [20]. This was extended in Bhattacharyya *et al.* [21] to unsteady stagnation-point flow of a Newtonian fluid and heat transfer from a stretching sheet with partial slip conditions. Niu *et al.* [22] investigated slip flow and heat transfer in a non-Newtonian nanofluid in a microtube. Khan *et al.* [23] analyzed the effects of hydrodynamic and thermal slip boundary conditions on double-diffusive free convective flow of a nanofluid along a semi-infinite flat solid vertical plate. Ibrahim and Shankar [24] studied the effects of velocity, thermal and solutal slip condition on the MHD boundary layer flow of a nanofluid past a permeable stretching sheet. Mabood *et al.* [25] studied the MHD slip flow over a radiation stretching sheet by using the optimal homotopy asymptotic method.

Some thermal systems such as those encountered in reactor safety, combustion and solar collectors operate at moderate to very high temperatures. In such cases, the temperature-concentration dependence relation is nonlinear and the Soret effect is of immense important. Partha [26] studied natural convection in a non-Darcy porous medium with a nonlinear temperature-concentration-dependent density relation.

In this paper, we analyze the effects of momentum, temperature and solute slip on stagnation-point flow over a permeable stretching or shrinking sheet. We transform the governing partial differential equations into similarity equations which are then solved numerically. The effects of physical parameters on the flow, heat, mass and nanoparticle concentration are determined and presented graphically. In the present paper, we mainly focus on the effect of slip parameters on the governing system along with the nonlinear thermal convection. To the best of authors knowledge such study has not been reported earlier in the literature.

2 Mathematical formulation

Consider steady, incompressible two dimensional boundary layer flow near the stagnation point in a permeable stretching or shrinking sheet. The x-axis is along the plate, the y-axis is measured normal to the plate. The temperature T, solute concentration S, and nanoparticle concentration C at the wall are denoted by T_w, S_w, and C_w, respectively, and their ambient values are T_∞, S_∞, and C_∞, respectively, where $T_w > T_\infty$, $S_w > S_\infty$, and $C_w > C_\infty$, and hence a momentum, thermal, solute, and nanoparticle concentration boundary layer form near the wall (Figure 1). We assume that hydrodynamic, thermal, and solute slip occur at the fluid-solid interface. Using the above assumption and the Oberbeck-Boussinesq approximation, the boundary layer equations are written as

$$\frac{\partial u}{\partial x} + \frac{\partial v}{\partial y} = 0, \tag{1}$$

Figure 1 Schematic diagram of the problem.

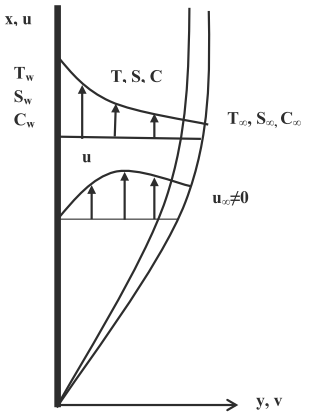

$$
\begin{aligned}
&u\frac{\partial u}{\partial x} + v\frac{\partial u}{\partial y} \\
&\quad = u_e\frac{du_e}{dx} + v\frac{\partial^2 u}{\partial y^2} + \frac{v}{K}(u_e - u) - \frac{(\rho_p - \rho_f)Kg}{\mu}(C - C_\infty) \\
&\qquad + \frac{(1 - S_\infty)\rho_f Kg}{v}\left[\beta_0(T - T_\infty) + \beta_1(T - T_\infty)^2 + \beta_2(S - S_\infty) + \beta_3(S - S_\infty)^2\right], \qquad (2)
\end{aligned}
$$

$$
u\frac{\partial T}{\partial x} + v\frac{\partial T}{\partial y} = \alpha_m\frac{\partial^2 T}{\partial y^2} + \tau D_B\frac{\partial T}{\partial y}\frac{\partial C}{\partial y} + \tau\frac{D_T}{T_\infty}\left(\frac{\partial T}{\partial y}\right)^2, \qquad (3)
$$

$$
u\frac{\partial S}{\partial x} + v\frac{\partial S}{\partial y} = D_S\frac{\partial^2 S}{\partial y^2} + \left(\frac{D_m K_T}{T_m}\right)\frac{\partial^2 T}{\partial y^2}, \qquad (4)
$$

$$
u\frac{\partial C}{\partial x} + v\frac{\partial C}{\partial y} = D_B\frac{\partial^2 C}{\partial y^2} + \left(\frac{D_T}{T_\infty}\right)\frac{\partial^2 T}{\partial y^2}, \qquad (5)
$$

and the corresponding boundary conditions are

$$
\begin{aligned}
&u = cx + L(\partial u/\partial y), \qquad v = 0, \qquad T = T_w + k_1(\partial T/\partial y), \qquad S = S_w + k_2(\partial S/\partial y), \\
&C = C_w, \quad \text{at } y = 0, \\
&u \to u_e(x) = ax, \qquad T \to T_\infty, \qquad S \to S_\infty, \qquad C \to C_\infty, \quad \text{as } y \to \infty,
\end{aligned} \qquad (6)
$$

u and v are the velocity components along the x- and y- directions, respectively, $u_e(x) = ax$ is the ambient velocity of the fluid, a is a constant, ν, ρ_f, and μ are the kinematic viscosity, density, and apparent viscosity of the base fluid, ρ_P is the density of the nanoparticle, K is the permeability of the porous medium, g is the acceleration due to gravity, β_1 and β_2 are the volumetric thermal expansion coefficient, respectively, β_3 and β_4 are the volumetric solute expansion coefficient, respectively, α_m is the effective thermal diffusivity, $\tau = \frac{(\rho c)_p}{(\rho c)_f}$, $(\rho c)_p$, and $(\rho c)_f$ are the volumetric heat capacity for nanoparticle and fluid, respectively, D_B and D_T are the Brownian and thermophoresis diffusion coefficients, respectively, D_s and D_m are the solute and mass diffusivities, respectively, K_T is the thermal diffusion ratio, c is a constant, L, k_1, and k_2 are the hydrodynamic, thermal, and solute slip factors, respectively.

We introduce the following similarity variables (see Ibrahim and Shankar [24]):

$$\psi = \sqrt{a\nu}xf(\eta), \quad \eta = \sqrt{\frac{a}{\nu}}y, \quad \theta = \frac{T - T_\infty}{T_w - T_\infty}, \quad \chi = \frac{S - S_\infty}{S_w - S_\infty}, \quad \phi = \frac{C - C_\infty}{C_w - C_\infty}, \tag{7}$$

where ψ is the stream function, which is defined in the usual way as $u = \partial\psi/\partial y$ and $v = -\partial\psi/\partial x$. Using the similarity variables, the governing equations are written as

$$f''' + ff'' + 1 - f'^2 + K_p(1 - f') + \lambda\left[(1 + \lambda_1\theta)\theta + Nc(1 + \lambda_2\chi)\chi - Nr\phi\right] = 0, \tag{8}$$

$$\theta'' + Pr\left(f\theta' + Nb\theta'\phi' + Nt\theta'^2\right) = 0, \tag{9}$$

$$\chi'' + Lnf\chi' + Sr\theta'' = 0, \tag{10}$$

$$\phi'' + Lef\phi' + \left(\frac{Nt}{Nb}\right)\theta'' = 0, \tag{11}$$

and the boundary conditions are written as

$$\begin{aligned} &f'(0) = \alpha_1 + \alpha_2 f''(0), \quad \theta(0) = 1 + \alpha_3\theta'(0), \quad \chi(0) = 1 + \alpha_4\chi'(0), \quad \phi(0) = 1, \\ &f'(\infty) = 1, \quad \theta(\infty) = 0, \quad \chi(\infty) = 0, \quad \phi(\infty) = 0. \end{aligned} \tag{12}$$

In the above equations, $K_p = \nu/aK$ is a parameter which is inversely proportional to the permeability K, $\lambda = Gr_x/\hat{Re}_x^2$ is the mixed convection parameter, Gr_x is the Grashof number, Re_x is the Reynolds number, Nc is the regular buoyancy parameter, λ_1 and λ_2 are the volumetric nonlinear thermal and solute constants, respectively, Nr is the buoyancy ratio parameter, Pr is the Prandtl number, Nb is the Brownian parameter, Nt is the thermophoresis parameter, Le is the Lewis number, α_1 is the velocity ratio or stretching ratio, α_2, α_3, and α_4 are momentum, thermal, and solute slip, respectively. These parameters are defined as

$$\begin{aligned} &Gr_x = \frac{(1 - S_\infty)\rho Kg(T_w - T_\infty)\beta_0 x^3}{\nu^3}, \qquad \hat{Re}_x = \frac{u_e(x)x}{\nu}, \qquad Nc = \frac{\beta_2(S_w - S_\infty)}{\beta_0(T_w - T_\infty)}, \\ &\lambda_1 = \frac{\beta_1(T_w - T_\infty)}{\beta_0}, \qquad \lambda_2 = \frac{\beta_3(S_w - S_\infty)}{\beta_2}, \qquad Nr = \frac{(\rho_p - \rho_f)(C_w - C_\infty)}{\rho_f(1 - S_\infty)\beta_0(T_w - T_\infty)}, \\ &Pr = \frac{\nu}{\alpha_m}, \qquad Nb = \frac{\tau D_B(C_w - C_\infty)}{\nu}, \qquad Nt = \frac{\tau D_T(T_w - T_\infty)}{\nu T_\infty}, \\ &Le = \frac{\alpha_m}{\varepsilon D_B}, \qquad \alpha_1 = c/a, \qquad \alpha_2 = \sqrt{a/\nu}L, \qquad \alpha_3 = k_1\sqrt{a/\nu}, \qquad \alpha_4 = k_2\sqrt{a/\nu}. \end{aligned}$$

The parameters of practical interest are the skin friction, local Nusselt number Nu_x, the local Sherwood number Sh_x, and the local nanoparticle Sherwood number Nn_x. These parameters are defined as

$$C_f = \frac{x\tau_w}{\rho u_e^2}, \quad Nu_x = \frac{xq_w}{k(T - T_\infty)}, \quad Sh_x = \frac{xq_s}{D_S(S - S_\infty)}, \quad Nn_x = \frac{xq_n}{D_B(C - C_\infty)}, \tag{13}$$

where $\tau_w = \mu(\frac{\partial u}{\partial y})_{y=0}$, $q_w = -k(\frac{\partial T}{\partial y})_{y=0}$, $q_s = -D_S(\frac{\partial S}{\partial y})_{y=0}$, $q_n = -D_B(\frac{\partial C}{\partial y})_{y=0}$.

Using the above non-dimensionless and similarity transformation we get

$$\begin{aligned} &Re_x^{1/2} C_f = f''(0), \qquad Re_x^{-1/2} Nu_x = -\theta'(0), \\ &Re_x^{-1/2} Sh_x = -\chi'(0), \qquad Re_x^{-1/2} Nn_x = -\phi'(0), \end{aligned} \tag{14}$$

where $Re_x = u_e(x)x/\nu$ is the local Reynolds number.

3 Results and discussion

The system of ordinary differential equations (8)-(11) along with boundary conditions (12) are integrated numerically by first choosing suitable initial guess values for $f(0)$, $f''(0)$, $\theta'(0)$, $\chi'(0)$, and $\phi'(0)$ to match the boundary conditions at ∞. Matlab `bvp4c` solver was used to integrate the system of equations. To verify the accuracy of the numerical results, we compared our results with those reported by Noghrehabadi *et al.* [27] as shown in Table 1. The results are in very good agreement, thus lending confidence to the accuracy of the present results.

A representative set of graphical results for the velocity, temperature, solute concentration and nanoparticle volume fraction as well as the skin friction, local Nusselt number, local Sherwood number and local nanoparticle Sherwood number is presented and discussed for different parametric values. We note that solutions of equations (8) and (11) exist for all values of $\alpha_1 > 0$, while in the case of a shrinking surface ($\alpha_1 < 0$), the equations have a solution only in the range $\alpha_1 > \alpha_{1\text{crit}}$, where $\alpha_{1\text{crit}}$ is a critical value of α_1. This critical value depends on other parameter values. There are no solutions real when $\alpha_1 < \alpha_{1\text{crit}}$. Dual solutions of the boundary layer equations appear in the range $\alpha_{1\text{crit}} < \alpha_1$. As noted by

Table 1 Comparison of the reduced Nusselt number $-\theta'(0)$ and Sherwood number $-\phi'(0)$ with Noghrehabadi *et al.* [27] for $Nc = 1$, $Nr = 3$, $\delta_1 = 1$, $Le = Pr = 10$. (a) $\delta_3 = \delta_4 = \lambda = \gamma = Ln = Sr = K_p = 0$ and (b) $\delta_3 = \delta_4 = \lambda = 0$, $Ln = 1$, $Sr = 0.5$, $K_p = 0.5$

δ_2	*Nb*	*Nt*	Noghrehabadi *et al.* [27]		Present (a)		Present (b)	
			Nur	Shr	Nur	Shr	Nur	Shr
0.0	0.1	0.1	0.952377	2.129394	0.95237683	2.12939377	1.00058819	2.66004285
		0.3	0.520079	2.528638	0.52007905	2.52863816	0.54419785	3.46549450
		0.5	0.321054	3.035142	0.32105433	3.03514247	0.31586598	4.38704894
	0.2	0.1	0.505581	2.381871	0.50558141	2.38187064	0.54400672	2.85986019
		0.3	0.273096	2.655459	0.27309580	2.65545946	0.28254157	3.33932740
		0.5	0.168077	2.888339	0.16807658	2.88833918	0.16127263	3.75314398
	0.3	0.1	0.252156	2.410019	0.25215609	2.41001880	0.27177120	2.86844013
		0.3	0.135514	2.608819	0.13551419	2.60881871	0.13604735	3.19990440
		0.5	0.083298	2.751875	0.08329860	2.75187540	0.07566950	3.45202615
1.0	0.1	0.1	2.751875	1.607430	0.71892800	1.60743180	1.14988755	3.00376688
		0.3	0.392596	1.908809	0.39259606	1.90881247	0.63804840	3.78822390
		0.5	0.242357	2.291156	0.24235674	2.29116127	0.37823785	4.77292460
	0.2	0.1	0.381652	1.798019	0.38165211	1.79802095	0.63400147	3.28337188
		0.3	0.206154	2.004545	0.20615392	2.00454704	0.33706394	3.78349666
		0.5	0.126877	2.180339	0.12687726	2.18034274	0.19696830	4.23378793
10.0	0.1	0.1	0.412468	0.922099	0.41247939	0.92225151	1.20480363	3.13488626
		0.3	0.225245	1.094883	0.22524897	1.09516618	0.67291837	3.91228460
		0.5	0.139050	1.314098	0.13905033	1.31453566	0.40123365	4.91834227
	0.2	0.1	0.218955	1.031454	0.21896995	1.03160059	0.66701497	3.44165247
		0.3	0.118275	1.149881	0.11827923	1.15009326	0.35709376	3.94942212
		0.5	1.204555	1.250672	0.07279486	1.25095500	0.21002703	4.41174227
	0.3	0.1	0.109199	1.043650	0.10921014	1.04379192	0.33770638	3.47832715
		0.3	0.058689	1.129708	0.05869191	1.12989321	0.17488396	3.84292518
		0.5	0.036078	1.191622	0.03607706	1.19185182	0.10098316	4.12849783

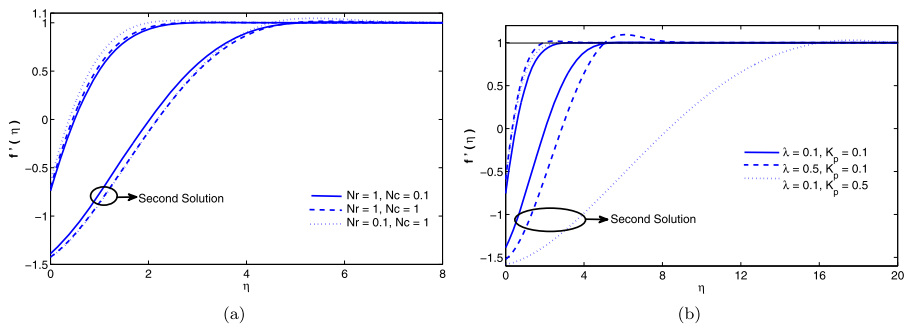

Figure 2 Effect of the velocity as a function of (a) *Nc*, *Nr* ($\lambda = 1$, $K_p = 0.1$), (b) λ, K_p ($Nc = Nr = 0.1$) with $\lambda_1 = \lambda_2 = Nt = Nb = 0.1$, $Pr = 0.5$, $Ln = Le = 1$, $Sr = 0.5$, $\alpha_1 = -1.6$, $\alpha_2 = 0.5$, $\alpha_3 = \alpha_4 = 0.1$.

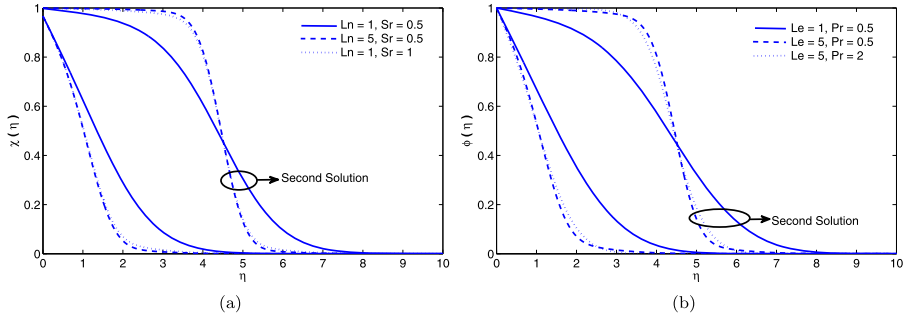

Figure 3 Solute concentration as a function of *Ln*, *Sr* ($Le = 1$, $Pr = 0.5$) (a) and (b) nanoparticle concentration as a function of *Le*, *Pr* ($Ln = 1$, $Sr = 0.5$) with $K_p = \lambda = \lambda_1 = \lambda_2 = Nr = Nc = 0.1$, $\alpha_1 = -1.6$, $\alpha_2 = 0.5$, $\alpha_3 = \alpha_4 = 0.1$.

Merkin [28], Postelnicu and Pop [29], the first solution is stable and physically realizable, while the second solution is unstable. In this study our primary focus is on the dual solutions and the effects of the slip coefficients and nonlinear volumetric thermal and solute constants.

The influence of the parameters Nr, Nc, λ, and K_p on the velocity profiles is shown in Figure 2. Dual solutions are observed in both instances. We note that the buoyancy ratio parameter has the effect of decelerating the fluid flow along the surface. This is reflected by the decrease in the fluid velocity in the vicinity of the surface. Hence the momentum boundary layer thickness decreases with an increase in Nr. The regular buoyancy ratio parameter Nc is similar to Nr and hence the momentum boundary layer thickness decreases with an increase in Nc. The parameter K_p is inversely proportional to the permeability of the medium K, hence the porous medium drag increases with K and so the velocity of the fluid increases with K_p. The momentum boundary layer thickness increased with an increase in the mixed convection parameter. Dual solutions were obtained for the opposing flow when $\lambda < 1$.

Figure 3 shows the effect of the nanofluid Lewis number Ln, the Soret number Sr, the Lewis number Le and the Prandtl number Pr on the solute and the nanoparticle concentrations when the other parameters are fixed. The concentration boundary layer thickness decreases with an increase in the nanofluid Lewis number. This is because an increase in the nanofluid Lewis number causes a reduction in the mass diffusivity of the nanofluid

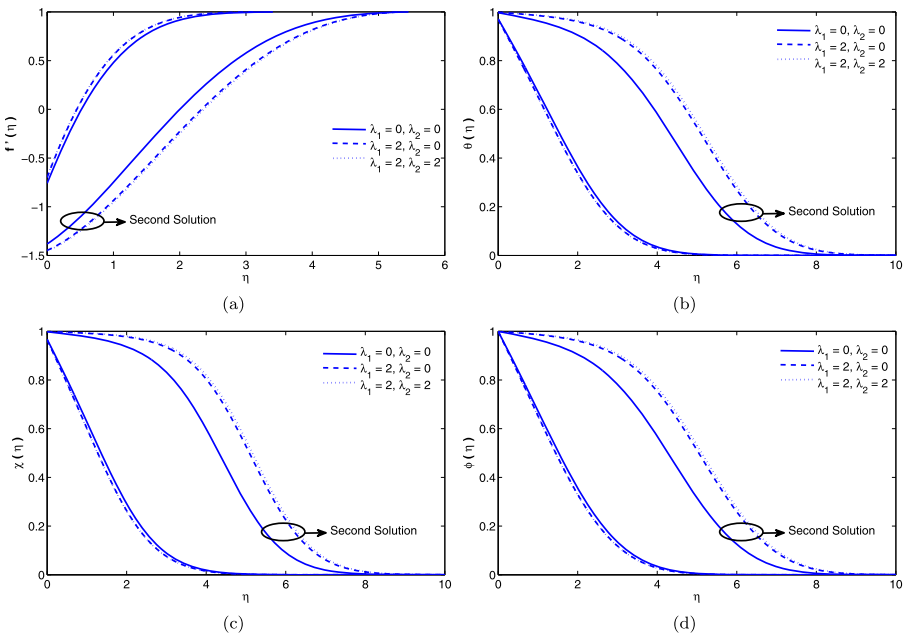

Figure 4 Effect of λ_1 and λ_2 on (a) velocity, (b) temperature, (c) solute concentration, and (d) nanoparticle concentration with $K_p = \lambda = Nr = Nc = 0.1$, $Le = Ln = 1$, $Pr = Sr = 0.5$, $\alpha_1 = -1.6$, $\alpha_2 = 0.5$, $\alpha_3 = \alpha_4 = 0.1$.

which in turn reduces the velocity of the fluid as well as the solute concentration. The solute concentration boundary layer thickness decreases with an increase in Ln while the nanoparticle volume fraction decreases with an increase in the Lewis number. The Prandtl number enhances the viscous diffusion rate which in turn reduces the velocity of the fluid and increases the concentration of the nanoparticle.

The effects of the nonlinear temperature and concentration coefficient on the velocity, temperature, solute concentration and nanoparticle concentration are shown in Figure 4. Dual solutions were obtained when $\alpha_1 = -1.6$ for all other parameter values. We observed that the effect of the convection nonlinearity (λ_1 and λ_2) is to reduce the thermal and solute boundary layer thicknesses. A similar observation was made by Partha [26]. This may partly be due to the nonlinear term enhancing the solute and nanoparticle density gradients near the wall. A careful observation shows that the effect of λ_1 is more significant compared with λ_2, particularly with respect to the momentum boundary layer profiles.

The slip coefficients have a significant influence on the velocity, temperature, solute, and nanoparticle concentration as clearly shown in Figure 5. The velocity of the nanofluid increases with momentum slip constant α_2. This is because momentum slip enhances the velocity at the fluid-solid interface. In the case of the no-slip condition, the fluid velocity adjacent to a solid surface is equal to the velocity of the stretching sheet *i.e.*, $f'(0) = \alpha_1 = 1$ while with an increase in other slip parameters, the momentum boundary layer thickness decreases. The thermal slip coefficient mainly affects the temperature profile and reduces the temperature at the surface. With thermal slip, more heat is transferred leading to a reduction in surface temperature and this reduces the velocity of the nanofluid. As a result both solute and nanoparticle concentration thickness decreases. The solute concentration

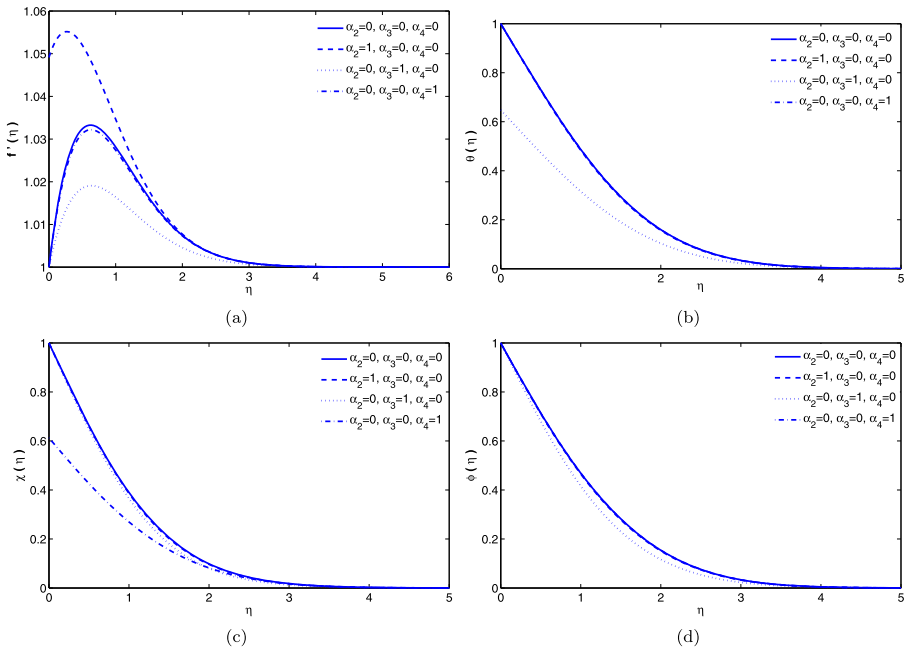

Figure 5 Effect of α_2, α_3, and α_4 on (a) velocity, (b) temperature, (c) solute concentration, and (d) nanoparticle concentration with $K_p = \lambda = \lambda_1 = \lambda_2 = Nr = Nc = 0.1$, $Le = Ln = 1$, $Pr = Sr = 0.5$, $\alpha_1 = 1$.

Figure 6 Local Nusselt number as a function *Kp* with $\lambda = 1$, $Nt = Nb = Nr = Nc = 0.1$, $Pr = 0.5$, $Ln = Le = 1$, $Sr = 0.5$, $\alpha_1 = \alpha_2 = \alpha_3 = \alpha_4 = 0.1$.

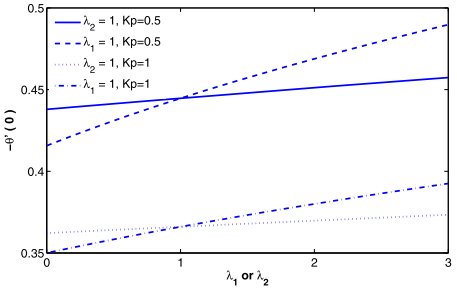

is mainly affected by the solute slip coefficient and the thickness of the solute concentration decreases with increase of the solute slip coefficient.

Figures 6 and 7 show the Nusselt number, Sherwood number, and density of the nanoparticle as a function of nonlinear thermal and solute constants for different values of K_p. With an increase in the permeability parameter, the velocity of the fluid reduces, hence as K_p increases, the surface temperature gradient, solute, and the nanoparticle concentration at the surface decrease which helps to reduce the local Nusselt number, local Sherwood number, and local nanoparticle Sherwood number. It evident that nonlinearity of the temperature and solute concentration both enhance the local Nusselt number and the local Sherwood number. This may be due to the fact that the nonlinearity term increases the temperature and concentration of the solute at the surface. A similar behavior is observed in the case of the nanoparticle concentration. It is interesting to note that the nonlinear curves are highly influenced by the nonlinear convection parameter as compared to the nonlinear concentration parameter.

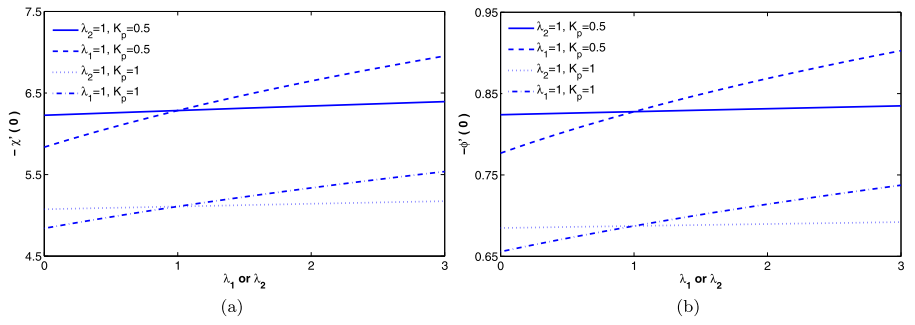

Figure 7 Effects of nonlinear thermal and solute constants on (a) local Sherwood number and (b) local density of nanoparticles as a function *Kp* with $\lambda = 1$, $Nt = Nb = Nr = Nc = 0.1$, $Pr = 0.5$, $Ln = Le = 1$, $Sr = 0.5$, $\alpha_1 = \alpha_2 = \alpha_3 = \alpha_4 = 0.1$.

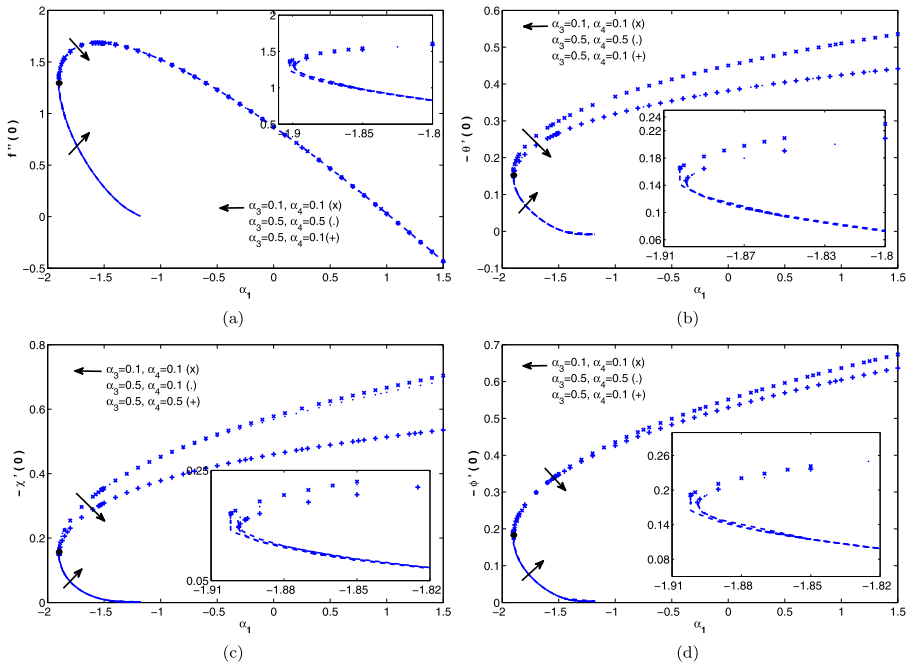

Figure 8 Effect of the slip constants on (a) skin friction, (b) local Nusselt number, (c) local Sherwood number, and (d) local density of nanoparticle with $K_p = 0.1$, $\lambda = \lambda_1 = \lambda_2 = 1$, $Nt = Nb = Nr = Nc = 0.1$, $Pr = 0.5$, $Ln = Le = 1$, $Sr = 0.5$, $\alpha_2 = 0.5$.

Figure 8 shows the skin friction, local Nusselt number, local Sherwood number, and local nanoparticle Sherwood number for different values of the thermal and solute slip constants. Here $\alpha_2 = 0.5$ is kept constant. As seen in Wang [30], in the case of the no-slip boundary conditions (*i.e.*, $\alpha_2 = \alpha_3 = \alpha_4 = 0$), the solution is unique for $\alpha_1 > -1$, there exist dual solutions for $-1.2465 \leq \alpha_1 \leq -1$, and no solution is found when $\alpha_1 < -1.2465$. The first solution is shown by marker while the second solution by the dotted line. With slip conditions, the range of α_1 values for which a unique solution as well as dual solutions exists significantly increases. The increased range of values of α_1 depends principally on the momentum slip coefficient. The critical values of α_1 are shown in Table 2. The critical value of α_1 decreases from –1.902 to –1.899 when the thermal slip coefficient increases

Table 2 Value of critical velocity ratio α_1 for different momentum, thermal, and solute slip constants for $Kp = \lambda_1 = \lambda_2 = Nt = Nb = Nc = Nr = 0.1$, $Pr = 0.5$, $Le = Ln = 1$, $Sr = 0.5$

$(\alpha_1)_{crit}$	α_2	α_3	α_4	dual solution range
−1.902	0.5	0.1	0.1	−1.902, −1.18
−1.899	0.5	0.5	0.1	−1.899, −1.18
−1.898	0.5	0.5	0.5	−1.898, −1.18
−2.622	1	0.1	0.1	−2.622, −1.18
−3.407	1.5	0.1	0.1	−3.407, −1.18

from 0.1 to 0.5. Similarly the critical α_1 decreases with an increase in the solute concentration. But the critical α_1 is enhanced by the momentum slip coefficient. It is observed that the lower limit of the critical α_1 is influenced more by the momentum slip parameter than by the thermal and concentration slip since it is part of the nanofluid velocity (see Figure 5(a)), which makes the system more unstable. A close observation shows that the dual solution region increases nonlinearly with increase of the momentum slip coefficient. The skin friction initially increases with momentum slip parameter but after a certain point (in this case $\alpha_1 = -1.56$) it decreases nonlinearly.

The local Nusselt number, local Sherwood number, and the local nanoparticle density are nonlinear increasing functions of the momentum slip parameter for the first solution while they are a decreasing function for the case of the second solution. It is interesting to note that the generation of vorticity for the shrinking velocity is reduced by an increase in the momentum slip at the surface (when $\alpha_1 > 1$). The momentum slip parameter enhances the velocity at the surface which forces the solute and particle to move away from the surface. As a result, the local Nusselt number, local Sherwood number, and local nanoparticle Sherwood number increase nonlinearly with the momentum slip parameter but decrease with increases in the solute slip coefficient. It evident that the local Nusselt number decreases with increase of the partial thermal slip coefficient and this finding is similar to earlier results by Zheng *et al.* [31]. The nature of the second solution for the local Nusselt number, local Sherwood number, and local nanoparticle Sherwood number is quite similar and this mainly depends on the momentum slip coefficient rather than the other slip coefficient.

4 Conclusions

The effect of momentum, thermal, and solute slip on nonlinear convection boundary layer flow from a stretching and shrinking sheet has been investigated numerically. Analysis of stagnation-point slip flow from a shrinking sheet has shown that existence and uniqueness of the solution depends on the slip parameters, mainly the momentum slip and the velocity ratio parameter α_1. Dual solutions were obtained when the velocity ratio was less than a certain critical value. The region of existence of the dual solution increases with the slip parameters. The nonlinear temperature and concentration coefficients reduce the thermal and solute boundary layer thicknesses. The thermal slip coefficient reduces the momentum and thermal boundary layer thickness. The local Nusselt number, local Sherwood number, and local density of the nanoparticles increase nonlinearly with the convection coefficient.

Competing interests
The authors declare that they have no competing interests.

Authors' contributions
All authors contributed equally to the writing of this paper. All authors read and approved the final manuscript.

Author details
[1]School of Mathematics, Statistics and Computer Science, University of KwaZulu-Natal, Private Bag X01 Scottsville, Pietermaritzburg, 3209, South Africa. [2]Fluid Dynamics Division, School of Advanced Sciences, VIT University, Vellore, 632 014, India.

Acknowledgements
The authors are grateful to the University of KwaZulu-Natal for financial support.

Received: 20 October 2014 Accepted: 7 December 2015 Published online: 04 January 2016

References

1. Crane, LJ: Flow past a stretching plate. Z. Angew. Math. Phys. **21**, 645-647 (1970)
2. Dutta, BK, Roy, P, Gupta, AS: Temperature field in the flow over a stretching sheet with uniform heat flux. Int. Commun. Heat Mass Transf. **12**, 89-94 (1985)
3. Choi, SUS: Enhancing thermal conductivity of fluids with nanoparticles. In: Siginer, DA, Wang, HP (eds.) Developments and Applications of Non-Newtonian Flows, vol. 99. ASME, New York (1995)
4. Ebrahimi, S, Sabbaghzadeh, J, Lajevardi, M, Hadi, I: Cooling performance of a microchannel heat sink with nanofluids containing cylindrical nanoparticles (carbon nanotubes). Heat Mass Transf. **46**, 549-553 (2010)
5. Li, H, Liu, S, Dai, Z, Bao, J, Yang, Z: Applications of nanomaterials in electrochemical enzyme biosensors. Sensors **9**, 8547-8561 (2009)
6. Shaw, S, Murthy, PVSN: The effect of shape factor on the magnetic targeting in the permeable microvessel with two-phase Casson fluid model. J. Nanotechnol. Eng. Med. **2**, 041003 (2011)
7. Huh, D, Matthews, BD, Mammoto, A, Montoya-Zaval, M, Hsin, NY, Ingber, DE: Reconstituting organ-level lung functions on a chip. Science **328**, 1662-1668 (2010)
8. Das, SK, Choi, SUS, Yu, W, Pradeep, T: Nanofluids: Science and Technology. Wiley, Hoboken (2007)
9. Kameswaran, PK, Shaw, S, Sibanda, P, Murthy, PVSN: Homogeneous-heterogeneous reactions in a nanofluid flow due to a porous stretching sheet. Int. J. Heat Mass Transf. **57**, 465-472 (2013)
10. Mabood, F, Khan, WA, Ismail, AIM: MHD boundary layer flow and heat transfer of nanofluids over a nonlinear stretching sheet: a numerical study. J. Magn. Magn. Mater. **374**, 569-576 (2015)
11. Aziz, A: Hydrodynamic and thermal slip flow boundary layers over a flat plate with constant heat flux boundary condition. Commun. Nonlinear Sci. Numer. Simul. **15**, 573-580 (2010)
12. Nield, DA, Kuznetsov, AV: Forced convection with slip-flow in a channel or duct occupied by a hyper-porous medium saturated by a rarefied gas. Transp. Porous Media **64**, 161-170 (2006)
13. Thompson, PA, Troian, SM: A general boundary condition for liquid flow at solid surfaces. Nature **389**, 360-362 (1997)
14. Nguyen, NT, Wereley, ST: Fundamentals and Applications of Microfluidics. Artech House, London (2009)
15. Karniadakis, G, Beskok, A, Aluru, N: Microflows and Nanoflows. Fundamentals and Simulation. Springer, New York (2005)
16. Maxwell, JC: On stresses in rarefied gases arising from inequalities of temperature. Philos. Trans. R. Soc. Lond. **170**, 231-256 (1879)
17. Hak, GM: Flow physics. In: Gad-el-Hak, M (ed.) The MEMS Handbook. CRC Press, Boca Raton (2002)
18. Beavers, GS, Joseph, DD: Boundary condition at a naturally permeable wall. J. Fluid Mech. **30**, 197-207 (1967)
19. Hamdan, MA, Al-Nimr, MA, Hammoudeh, VA: Effect of second order velocity-slip/temperature-jump on basic gaseous fluctuating micro-flows. J. Fluids Eng. **132**, 074503 (2010)
20. Bhattacharyya, K, Mukhopadhyay, S, Layek, GC: Slip effects on boundary layer stagnation-point flow and heat transfer towards a shrinking sheet. Int. J. Heat Mass Transf. **54**, 308-313 (2011)
21. Bhattacharyya, K, Mukhopadhyay, S, Layek, GC: Slip effects on an unsteady boundary layer stagnation-point flow and heat transfer towards a stretching sheet. Chin. Phys. Lett. **28**, 094702 (2011)
22. Niu, J, Fu, C, Tan, W: Slip-flow and heat transfer of a non-Newtonian nanofluid in a microtube. PLoS ONE **7**, e37274 (2012)
23. Khan, WA, Uddin, MJ, Md Ismail, AI: Hydrodynamic and thermal slip effect on double-diffusive free convective boundary layer flow of a nanofluid past a flat vertical plate in the moving free stream. PLoS ONE **8**, e54024 (2013)
24. Ibrahim, W, Shankar, B: MHD boundary layer flow and heat transfer of a nanofluid past a permeable stretching sheet with velocity, thermal and solutal slip boundary conditions. Comput. Fluids **75**, 1-10 (2013)
25. Mabood, F, Khan, WA, Uddin, MJ, Md Ismail, AI: Optimal homotopy asymptotic method for MHD slips flow over a radiating stretching sheet with heat transfer. Far East J. Appl. Math. **90**, 21-40 (2015)
26. Partha, MK: Nonlinear convection in a non-Darcy porous medium. Appl. Math. Mech. **31**, 565-574 (2010)
27. Noghrehabadi, A, Pourrajab, R, Ghalambaz, M: Effect of partial slip boundary condition on the flow and heat transfer of nanofluids past stretching sheet prescribed constant wall temperature. Int. J. Therm. Sci. **54**, 253-261 (2012)
28. Merkin, JH: On dual solutions occurring in mixed convection in a porous media. J. Eng. Math. **20**, 171-179 (1985)
29. Postelnicu, A, Pop, I: Falkner-Skan boundary layer flow of a power-law fluid past a stretching wedge. Appl. Math. Comput. **217**, 4359-4368 (2011)
30. Wang, CY: Stagnation flow towards a shrinking sheet. Int. J. Non-Linear Mech. **43**, 377-382 (2008)
31. Zheng, L, Zhang, C, Zhang, X, Zhang, J: Flow and radiation heat transfer of a nanofluid over a stretching sheet with velocity slip and temperature jump in porous medium. J. Franklin Inst. **350**, 990-1007 (2013)